Title No. 118-M106

Three-Dimensional (3D)-Printed Wood-Starch Composite as Support Material for 3D Concrete Printing

by Viacheslav Markin, Christof Schröfl, Paul Blankenstein, and Viktor Mechtcherine

The applicability of wood-based, starch-bonded composite materials for three-dimensional (3D)-printed temporal, fully recyclable support structures was studied experimentally with respect to delivering the specific geometric and load-bearing features of the product of a continuous 3D concrete printing process. Extrudability of the support material developed was verified by direct test using a conventional screw extruder. The observations and quantitative results were compared with those gained with a ram extruder. The development of the compressive strength of the support materials was analyzed experimentally from an early age, beginning a few minutes after extrusion. The results obtained confirmed the sufficiency of the product's strength in withstanding prospective weight loads of concrete layers printed on top of the support. Furthermore, methods of enhancing early-age compressive strength were analyzed, and a most promising approach was experimentally implemented—namely, the deposition of the material under a constant defined airflow. In contrast to its promising mechanical material characteristics, massive fungi formation was observed as early as 1 day, amounting to a severe drawback. Consequently, improvements to the material's composition are suggested that will not impair the environmental sustainability of the support material.

Keywords: material development; support material; sustainability; three-dimensional (3D) concrete printing.

INTRODUCTION

Three-dimensional (3D) printing with cement-based building materials has been intensively researched for several years. Both materials and process technology have been analyzed and developed further,[1-3] and accordingly, 3D concrete printing (3DCP) has evolved from a mere idea to a practicable production technique with pilot structures already in existence.[4]

A holistic view of 3DCP reveals four significant potential advantages compared with traditional concrete production: increased productivity, lower costs, time savings, and freedom of form and design.[5] The last advantage, however, has certain limitations. Cantilevered or horizontal self-supporting structures, quite naturally, cannot be built because extra inlays of prefabricated, supporting formwork may markedly slow the construction progress and dramatically increase its costs. Thus, feasible solutions for the production of such overhanging structures and lintels over windows and doors also need to be developed. So far, only a few approaches to address this challenge have been implemented.[6-10] Figure 1 shows, for example, manually installed doorway lintels that can be made of various materials. However, interruptions in the construction process and the involvement of additional labor for the manual installation of the lintels contradict the key idea of automation in construction and continuous 3DCP.[12]

Figure 1 also illustrates a more promising concept for the production of overhanging structures. With the help of a robot, the prefabricated window frame is placed at the predefined location and held until the surrounding walls are printed.[6] Depending on the size and weight of the window frame and the structural buildup rate, and the resulting load-bearing capacity of the concrete, fixation of the frame is needed either for several minutes or, in certain cases, for hours. Furthermore, more than one additional robot will most likely be needed to continuously print wall elements with several windows.

As further shown in Fig. 1, it is possible to produce self-bearing arches by a slight lateral shift of the concrete layers.[11] The emerging structural shape was once typical in Indian, Islamic, and Gothic architecture. However, this building technique significantly restricts design flexibility.

Another study proposed the use of a 3DCP machine printhead with a specially designed, automated gripper that could install a prefabricated lintel at a specified position in the wall.[9] As soon as the gripper completes the lintel installation, the printhead can begin depositing the subsequent layers on top. However, a significant drawback of this solution is assumed to lie in the potentially enhanced vulnerability to crack formation in the wall. The rigid lintel beam restrains the upper layer, which shrinks over time owing to desiccation and cement hydration, thus giving rise to such cracking. Another presumable drawback is the distinct deformation of the concrete layers induced by the additional weight of the lintel.

Tay et al.[10] proposed the use of concrete as a building material for structural elements and at the same time as support material (SM). By decreasing the flow rate in the regions of the planned openings, weaker but still adequate load-bearing layers could be produced, and the regular concrete layers could subsequently be placed on top of such support. The weaker regions can later be easily cut out of the structural element. This method may be used for small subtasks, such as the provision of holes for electrical conduits or pipes. However, this approach does not include a concept for reusing the severed pieces of hardened concrete.
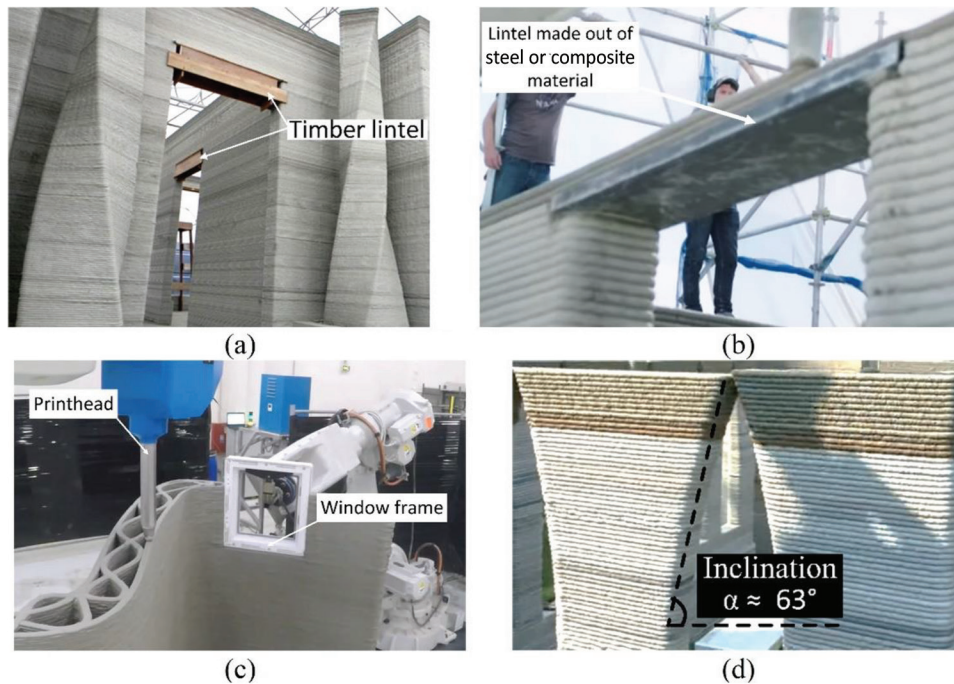
Fig. 1—Examples of production of overhanging structures: (a) 3D-printed hotel villa[8]; (b) 3DCP of apartment building at ICON[7]; (c) automated installation of window frame[6]; and (d) 3DCP of inclined elements.[11]

Similar to fused deposition modeling 3D printing (FDM 3DP), support structures can be printed to stabilize overhangs or parts suspended in midair. When the concrete in the structure itself is sufficiently hardened, the support structures are removed and fully recycled.[13] Process-specific parameters that distinguish 3DCP from other methods in additive manufacturing are also summarized.[3,14,15] The authors have described the first successful effort to develop a sustainable SM for extrusion-based digital construction (DC).[16] The SM was based on wood, starch, and water only. It was completely bio-based and regarded as fully recyclable. Material and process-specific requirements for the integration of this SM into 3DCP based on extrusion-based DC were identified. A feasible process chain for the mixture design approach was established. The cited study demonstrated the basic influences of the composition of the SM on extrudability and compressive strength. However, the extrudability was not sufficiently characterized and classified, and the shape stability of the SM was not assessed.

The present paper aims to evaluate whether the wood-starch-based SM studied previously applies to the production of overhangs and strongly inclined structures. The generation and 3D printing of the SM should be fully integrated into the continuous workflow of 3DCP. Important issues include the determination of the process steps influencing the life cycle of the SM and its practically relevant material properties. Figure 2 shows the process chain for the 3D printing of SM. The major steps are as follows: 1) 3D printing of the SM; 2) demolishing the SM after sufficient hardening of the supported concrete; 3) temporary storage; and 4) reprocessing. In addition, reprocessing should be followed by constant quality control. The investigation at hand focuses on step 1, especially on the properties of the SM relevant for
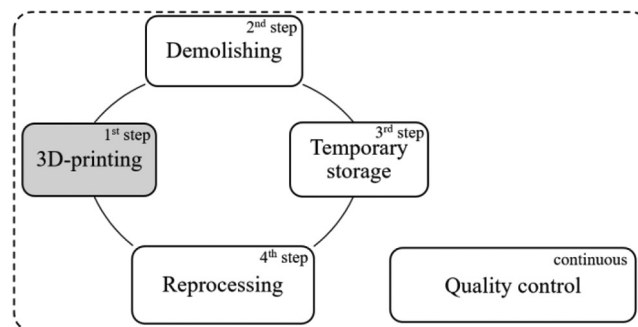

Fig. 2—Process chain for application of SM.

3D printing. Important properties of the SM are its economic and environmental sustainability, which are delivered by wood-binder compounds without restriction. Maize starch was chosen as the binder due to its advantageous characteristics in cohesion and flow behavior in the fresh state.[16,17] Prior to the experimental work, the required strength and load-bearing capacity of the SM were determined.

RESEARCH SIGNIFICANCE
The development of formwork-free DC using concrete emerged into civil engineering practice several years ago. 3DCP based on additive manufacturing—that is, layer-by-layer material deposition—promises high flexibility in terms of the geometry of elements to be produced and related printing strategies. However, a severe drawback of this technology is its limited ability to execute overhangs and strongly inclined structures smoothly and as an integral part of the automated, continuous printing process. The current study assesses the potential of wood-starch-based compound for the application as a printable, fully biologically based, recyclable SM for 3DCP.

Table 1—Mixture compositions for the support material, per m³

Unit content, kg/m³	M-1	M-2	M-3
Spruce particles Type A	71.4	35.7	30.8
Spruce particles Type B	—	35.7	30.8
Maize starch	154.7	152.8	121.5
Guar flour	39.9	39.2	32.9
Tap water	552	545	607
Water-reducer (aqueous solution as obtained)	—	14.6	29.1

Table 2—Mixture composition of printable concrete, per m³

Constituents	Density	Weight per unit volume, kg/m³
CEM I 52.5 R ft.	3100	391
Fly ash	2271	213
MSS[*]	1400	213
Sand 0.06-0.2	2650	252
Sand 0-1	2650	252
Sand 0-2	2650	756
Tap water	1000	138
Superplasticizer PCE	1010	14

[*]Aqueous suspension of microsilica with dry mass content of 50 ± 2%.

Fig. 3—Light microscope pictures of spruce particles used: (a) maximum sieve size 0.5 mm; and (b) maximum sieve size of 2.0 mm.

Fig. 4—Granulation of SM for ensuring of continuous material feeding: (a) sieves used for manual granulation of SM; and (b) granulated SM (scale in cm).

Fig. 5—Schematics of equipment used for printing trials: (a) screw extruder; and (b) ram extruder.

EXPERIMENTAL PROCEDURE

Raw materials and mixture design

Table 1 presents the mixture proportions for the SM under investigation. For 3DCP experiments, that is, for integrating the SM deposition into the continuous workflow, the finely grained concrete mixture described earlier[18] was used (Table 2).

Two types of spruce particles were used as filler in all mixtures, which were produced at the Institut für Holztechnologie Dresden gemeinnützige, Dresden, Germany. Type A had a maximum particle size of 0.5 mm, defined by the sieve mesh size through which it passed, and type B had a particle size of 2.0 mm (refer to Fig. 3). Maize starch was used; guar flour was added to adjust the rheological properties of the SM; and a polycarboxylate-based high-range water-reducing admixture was used to achieve optimum consistency without a significant increase in water content.

Preparation

The components were mixed in a planetary mixer. For each test, 30 L of the SM were prepared. At first, all dry materials were homogenized for 2 minutes at an engine speed of 68 rpm. Subsequently, water and water reducers were added, and mixing was resumed for 2 more minutes at the same speed. After optical assessment of the homogeneity achieved and scraping of the walls, mixing was continued for 1 additional minute at the same speed. SM compositions exhibited stiff and non-flowable consistency similar to that of clay pastes. It was assumed that the granulation of the SM could facilitate continuous material feeding during the extrusion by a screw extruder. The granulation of the SM is shown in Fig. 4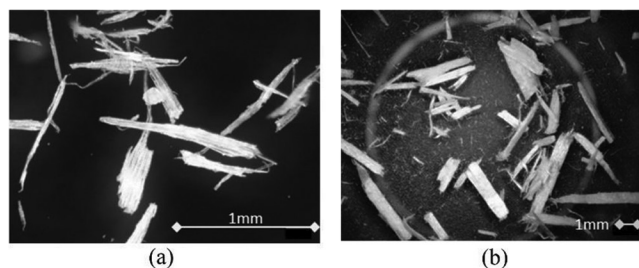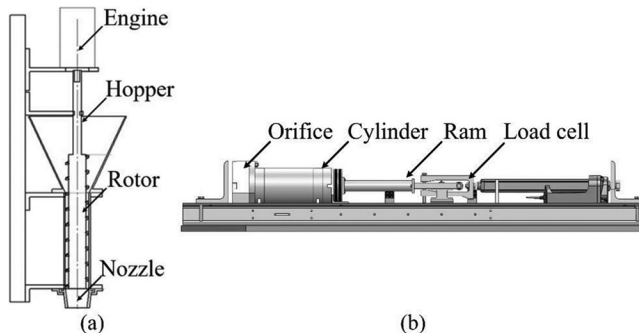. Mesh sizes of 8.0 and 4.0 mm were used for the granulation of the already prepared SM. The ratio of the two granules' fractions was held equal at 50:50. The entire mixing procedure took 4 minutes, and the granulation of the SM took less than 5 minutes.

Extruders for printing trials

Two devices were used to assess the extrudability of the SM: 1) a screw extruder; and 2) a ram extruder. Figure 5 shows the schematic construction of the customary screw extruder. The specific geometry of the Archimedes screw implemented allows a flow rate of 0.12 m³/h at a rotation speed of 0.5 rpm. Essentially, the difference between a screw and a ram extruder is the method of conveying the material. In a ram extruder, the material is pushed through the cylinder by a piston (refer to Fig. 5). Experiments were carried out in this study at a constant effective ram velocity of 15 mm/s, that is, at a constant flow rate. A load cell with a maximum load capacity of 5 kN was used to continuously measure the ram extrusion force (REF). The orifice of the ram extruder
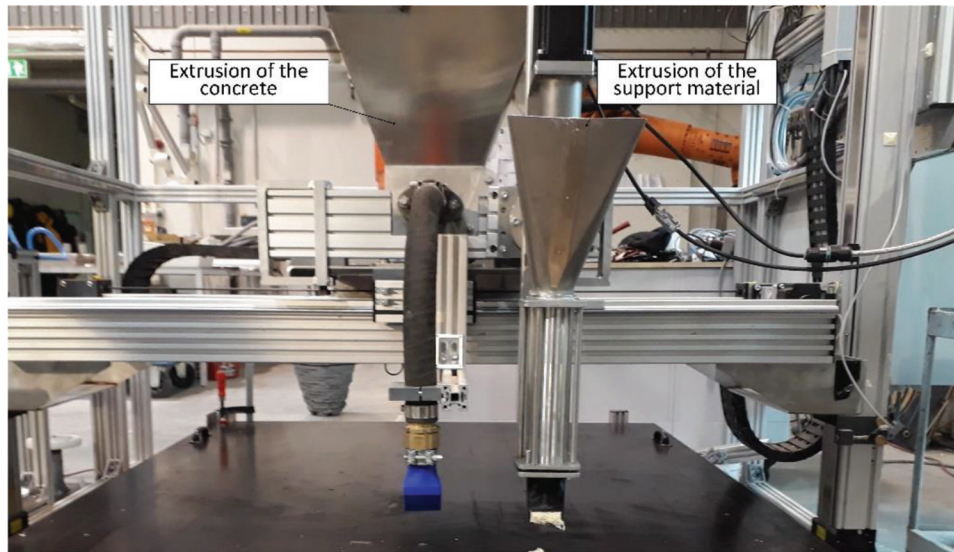
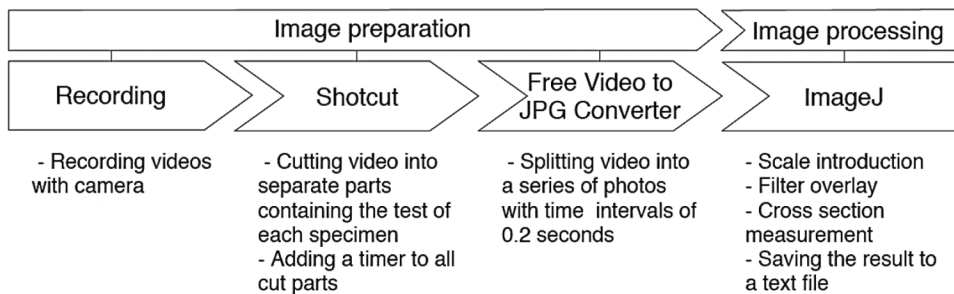*Fig. 6—Experimental setup for continuous 3D printing with concrete and SM.*

Fig. 7—Followed procedure for preparation and processing of images.[20]

had a diameter of 60 mm. After filling the SM into a cylinder of diameter 120 mm and height 300 mm, the REF and effective ram displacement were measured.

3D printing with support material and concrete

Figure 6 shows the test setup for the continuous 3D printing of SM and concrete. The SM was extruded with a screw extruder detailed in the previous section. The concrete mixture was extruded with a modified mortar pump, as extensively described previously.[19] Both extruders were rigidly connected and moved using the automatic gantry system at a constant speed of 40 mm/s. The concrete extruder and the SM extruder were each equipped with a rectangular nozzle with opening dimensions of 15 x 49.5 mm and 15 x 50 mm, respectively. The printable concrete mixture was prepared in parallel with the SM preparation. After mixing, the materials were filled into the respective hoppers of the printheads. Layer-by-layer deposition intervals for both concrete and SM layers were set at 30 seconds.

Uniaxial unconfined compression test

A displacement-controlled uniaxial, unconfined compression test (UCT) was performed on cylindrical SM specimens with a height of 34 mm and a diameter of 48 mm to determine early-age mechanical properties. The SM was placed in a cylindrical formwork and was manually compacted. The formwork was removed before the compression test. To

determine the influence of production methods, one batch was prepared directly from the 3D-printed filaments of the SM. Specimens were produced by extracting them from the 3D-printed filaments using a cylindrical, sharp, thin-walled cutter. The tests were performed using a testing machine equipped with a 10 kN load cell and loading plate with a diameter equal to that of the specimens. The loading rate was 30 mm/min; the test was stopped at a strain of 25%. The cross section of each specimen was assessed optically using images made with a digital single-lens reflex camera as the basis for calculating the stress values. To obtain a reasonable frequency of images for analysis, a video was recorded. This video was later converted into a sequence of single images using an open-source program. Image processing was performed using the methodology described by Invaniuk[20] (refer to Fig. 7).

Enhancement of early-age mechanical properties

Figure 8 depicts the proposed method for enhancing the early-age mechanical properties using airflow. To assess the effectiveness of this approach in the laboratory, two test series were prepared; one test series aimed at quantifying the mechanical properties of the untreated specimens as a reference. SM specimens were therefore kept under ambient conditions of approximately 60% relative humidity and temperature of 20°C and tested at the ages of 60 minutes, 180 minutes, and 24 hours after water was added during mixing. In the other
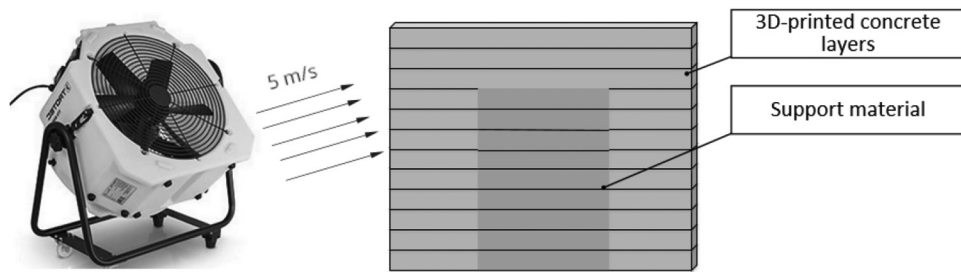
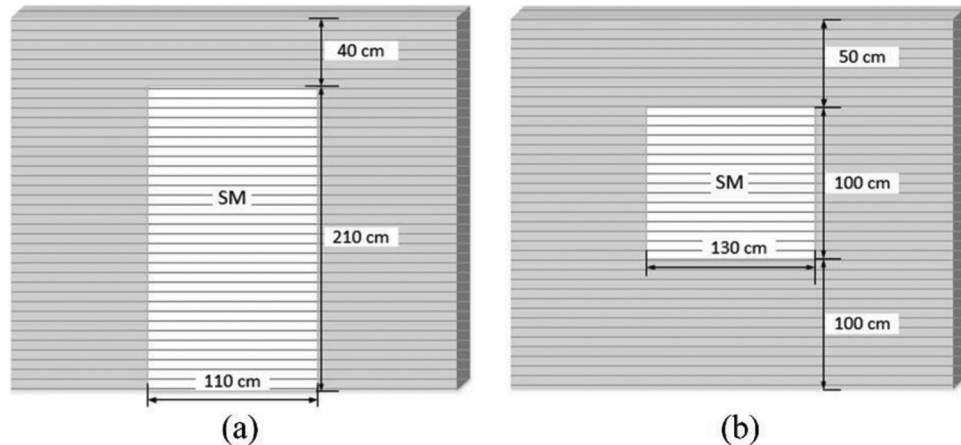Fig. 8—Concept to accelerate drying of SM on construction side.

Fig. 9—Two typical application scenarios for SM in 3DCP: (a) door opening with concrete cover of 40 cm; and (b) window opening with concrete cover of 50 cm.

series, conditions simulated those onsite by the use of a fan. Cylindrical SM specimens were placed in a wind tunnel with a constant airflow of 5 m/s, relative humidity of approximately 50%, and a temperature of 20°C at the age of 40 minutes after water addition. Technical information on the wind tunnel can be found in Ghourchian et al.[21] These specimens were treated in the wind tunnel for three durations—specifically 20 minutes, 120 minutes, and 24 hours. At least four individual specimens were tested per series.

Electron microscopy

An environmental scanning electron microscope was used in its so-called "low-vacuum mode." The specimens were imaged as obtained, with neither sputter coating nor excessive drying during the measurement procedure.

EXPERIMENTAL RESULTS AND DISCUSSION
Requirements on load-bearing capacity of SM

The mechanical properties of the SM must be adjusted with regard to the application scenario. Figure 9 shows two typical cases for the application of the SM: the production of a window and a door opening. The SM is exposed to stresses caused by its own weight, the weight of the subsequent SM filaments, and, finally, the weight of the subsequent concrete filaments. For simplicity in the case at hand, wind load during the construction process was neglected. The bottom layer of the SM structure is considered the most stressed layer owing to the accumulation of the weights of the upper layers, extruded and deposited later on. Therefore,

yield stress in the bottom layer of the SM structure depends primarily on the height of the printed support structure and on the height of the concrete structure. Thus, the stress in the bottom layer of the SM structure can be expressed by the following equation

$$E_{SM} = \rho_{SM} h_{SM} g + \rho_c h_c g \qquad (1)$$

where ρ_{SM} is the density of the SM; h_{SM} is the height of the SM structure; g is the gravity constant; ρ_c is the density of the concrete; and h_c is the height of the concrete layers.

It must be noted that Eq. (1) represents the worst case because it does not consider any redistribution of stresses within the system. In reality, a part of the load induced by concrete deposited above the SM is carried by concrete to the left and right of the opening, while—assuming contact between SM and concrete in a vertical plane—a part of the forces in SM would be redistributed to a stiffer material—that is, concrete again to the left and the right.

With an SM density of 1.100 kg/m³ and a concrete density of 2.200 kg/m³, the yield stress of the bottom layer of the SM structure would be maximally 0.03 MPa for a door opening and maximally 0.02 MPa for the window opening with the dimensions shown in Fig. 9. It is worth noting that according to results published on 3D printing with foam concrete, requirements for the early-age stress capacity of the SM could be significantly lower because the density of the foam concrete is noticeably lower than the density of ordinary 3D-printable concrete.[18-20]

Measurement of extrusion force by use of ram extruder

Figure 10 shows the REF measured at various ram displacements. All curves plotted can be divided into three distinct regions, confirming previous results on ram extrusion[18,22-24]: a) an exponential increase of REF at flow initiation; b) a steady-state region; and c) flow termination. Compositions M-2 and M-3 exhibited similar allocations of the exponential increase in the REF against the displacement. However, for M-1, the exponential increase in REF started much later than for the other two mixtures. The pronounced increase in REF is linked to the compaction of the material in the barrel of the extruder. A shift of the onset of the exponential increase in the REF from approximately 200 mm of ram displacement by M-2 and M-3 to approximately 240 mm for M-1 was observed. The absence of the water-reducer markedly influenced the density, porosity, and viscosity of M-1. The reason for this is the combination of spruce particles with differently sized particles in M-2 and M-3, which greatly enhanced packing density. Figure 10 indicates that M-1 has the highest REF and M-3 the lowest. In general, the REF of any mixture is inversely proportional to its extrudability. Hence, M-3 has the highest extrudability. It is worth noting that in the present context of extrusion-based DC, the term extrudability defines only the ability of the material to pass through the orifice of the extruder but says nothing about the ability of the material to retain the shape taken from the orifice. Thus, in addition to the assessment of mere extrudability, a quantitative estimation of the buildability of the SM is needed, for example, by measuring early-age mechanical properties.

3D printing test results

The results discussed in the previous section revealed that all SM compositions designed could be successfully extruded by the ram extruder. Figure 11 visualizes the example of SM extrusion by this device. Figure 11 shows a wall specimen consisting of SM filaments manually deposited layer by layer and obtained from the ram extruder. Each layer retained approximately the circular cross section imposed by the geometry of the orifice, resulting in insufficient contact surfaces between the layers, which would severely compromise the structural stability of the supporting parts. A rectangular cross section of the SM layers naturally appears more appropriate.

According to the plan, the suitability of the screw extruder equipped with a rectangular nozzle was tested as well. Figure 11(c) depicts an SM specimen printed by the screw extruder. It consisted of six layers, all of which had retained the rectangular shape imposed by the nozzle. No significant deficiencies in the quality of the individual layers could be noted. However, in contrast to the ram extruder, only composition M-3 could be extruded by this device, whereas M-1 and M-2 could not be handled.

A precondition for conveying the SM by a screw is that little to no adhesion of the material to the surfaces of the screw should take place. Whereas all SM compositions exhibited stiff and non-flowable consistency in a quite similar fashion to clay pastes, M-3 contained a water-reducing admixture and more water than M-1 and M-2, and
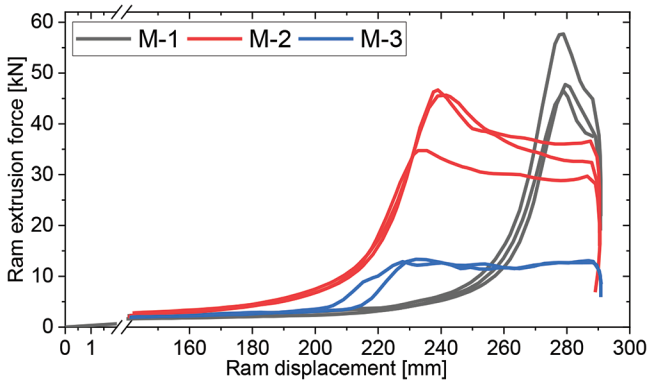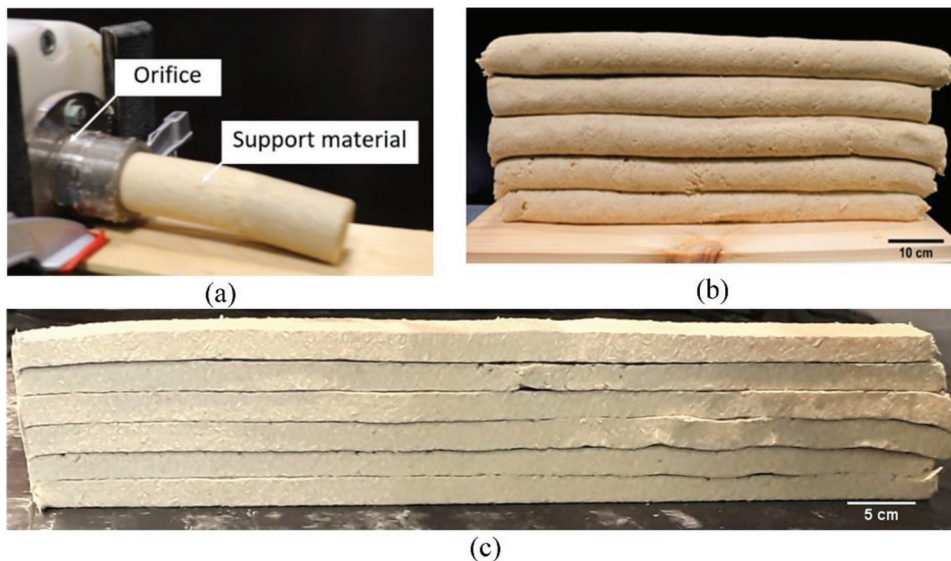

Fig. 10—Results of ram extrusion tests.

Fig. 11—Extrusion of SM: (a) extrusion by ram extruder with circular orifice; (b) manually assembled M-3 SM layers produced with ram extruder; and (c) SM wall specimen made of M-3 by layer-by-layer deposition using screw extruder with rectangular nozzle.
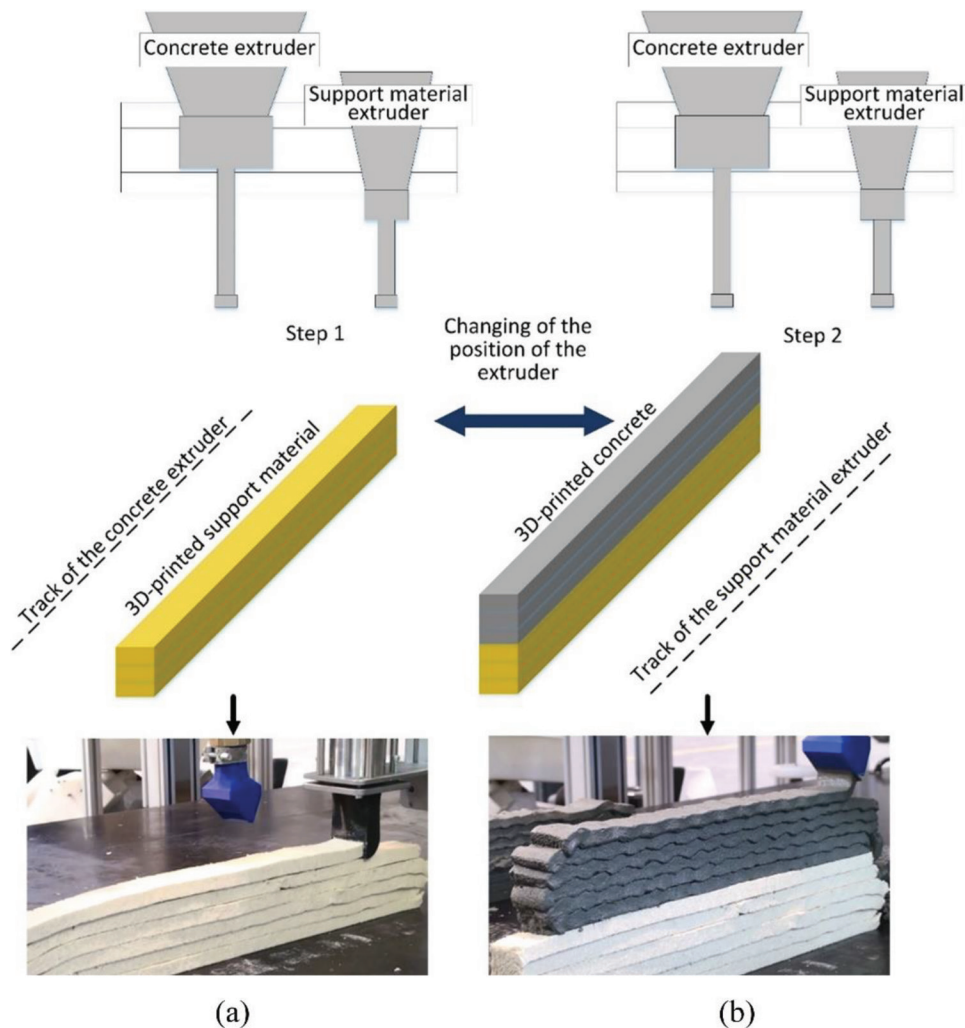
Fig. 12—(a) Scheme of integrated continuous 3D printing of SM and concrete; and (b) images of printed specimens. (Note: height of each layer was 15 mm; width of each layer was 50 mm.)

thus the "stickiness" of M-3 was less pronounced and its plasticity distinctly higher than that of the other two SM. Figure 10 indicates the ease of conveying M-3 with a ram extruder as compared with M-1 and M-2. This difference was significant with respect to the extrudability of M-3 by the screw extruder in the given configuration.

Interestingly, granulation of the SM proved insufficient in enhancing the conveying ability of any SM composition through the screw of the extruder when compared with the as-obtained material from the mixing process (refer to Fig. 4). To enhance the extrudability of the SM by the screw extruder, the material was compacted manually and pushed toward the screw using an auxiliary wooden bar, which pronouncedly facilitated the continuous extrusion. This finding may indicate the need for further developments with respect to the extruder unit.

Continuous 3D concrete printing with implemented SM deposition

The full-scale integrated 3D printing process of both SM (M-3) and concrete and the printing procedure's outcomes are illustrated in Fig. 12. Six SM layers were printed one after another; then, the positioning of the extruders was changed, and six concrete layers were deposited on top of the SM. While the flow rate of the SM matched the forwarding velocity of the extruder, the concrete flow rate was not accurately synchronized, resulting in smooth SM but slightly, yet visibly, buckled concrete layers. During the printing of the concrete, the filaments of the SM showed no visible deformations. However, approximately 5 minutes after completion of the concrete extrusion, deformation of the support structure began. Starting at the bottom layer, the stability of the overall structure was severely endangered. This observation emphasizes the significance of enhancing the early-age mechanical properties of the SM, as discussed in the next section.

Uniaxial unconfined compression test

The SM must develop sufficient mechanical strength to withstand the stresses from consecutive SM and concrete layers without exceeding permissible deformations. Yield stress and compressive strength of the SM increase over time, which is attributed to the evaporation of water and associated consolidation. Previous research on this starch-bonded SM shows that the moisture content greatly influences the compressive strength and its development over
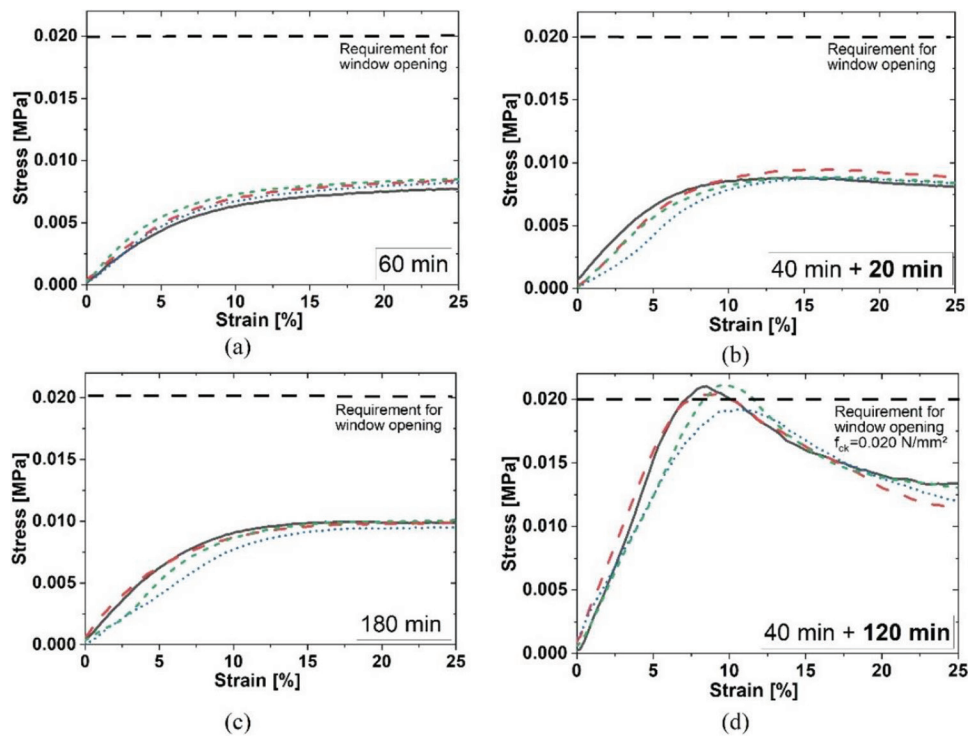
Fig. 13—Stress-strain diagrams obtained by unconfined compression test of composition M-3: (a) SM aged 60 minutes after water addition in ordinary room climate; (b) SM aged 40 minutes after water addition followed by 20 minutes of exposure in wind tunnel; (c) SM aged 180 minutes after water addition in ordinary room climate; and (d) SM aged 40 minutes after water addition followed by 120 minutes of exposure in wind tunnel.

time. Aside from the physical bonding of water molecules into the polysaccharide structures, water is not bound chemically, in contrast to the hydrating concrete/cement condition.[16] Hence, gains in yield stress and mechanical strength can be improved only by accelerating the drying process of the SM unless the composition of the SM is substantially changed. For example, installing a blower fan on the construction site will speed up the strength development of the SM due to the increased moisture transport by convection/air exchange (refer to Fig. 8). However, it needs to be considered that premature dehydration of the concrete layers would lead to increased capillary pressure and may result in crack formation owing to restrained plastic and/or drying shrinkage. Therefore, it is necessary to adapt the curing procedure so that concrete cracking is not triggered. One option would be to protect concrete against desiccation by applying thin polymer films on the concrete surface—for example, by spraying.

The results of the UCT are presented in Fig. 13. The stress-strain diagrams show that the properties of the SM change over time and depend on both curing time and curing conditions. While one set of cast specimens was cured without air movement in the ordinary laboratory climate, another was exposed to controlled airflow (that is, wind), as in Fig. 8. The aeration was started 40 minutes after SM preparation and lasted for 20 or 120 minutes, respectively (Fig. 13). Prolonged air circulation positively influenced the gain in mechanical properties of the SM. Distinct enhancement of the mechanical properties could be seen only after 120 minutes of wind curing, whereas 20 minutes of curing did not suffice. Interestingly, 20 minutes of wind curing resulted in fairly

similar load-carrying capacities to the no-wind conditions, but this value was obtained at lower strain values, indicating higher stiffness of the material. Contrarily, aerating the SM specimens for 120 minutes almost doubled their compressive strength; a value of 0.02 MPa was achieved, which had been calculated to be the minimum stress capacity required.

Continuous 3DCP of a wall element with a window opening is possible from this point of view. However, the peak stress value corresponds to a strain of 7.5% (refer to Fig. 13). In a window opening with a height of 1 m, such deformation of the support structure translates into an absolute deformation of approximately 7.5 cm, which is too high. Note, however, that this estimation is based on extremely conservative assumptions, as mentioned previously. In addition, it must be stated that any considerable deformation of SM in the vertical direction would certainly lead to corresponding lateral deformation in the horizontal direction, which the contiguous concrete walls would restrain. Such restrained deformation would induce a multi-axial state of stresses in the SM and considerably decrease its deformation in the vertical direction, thus increasing its compressive strength. A more comprehensive analysis of SM's in-place deformations and strength behavior is the subject of an ongoing investigation. Nevertheless, additional measures to reduce the deformability of SM might be needed, such as extending the duration of aeration.

Results of the UCT discussed so far stemmed from cast specimens for reasons of experimental feasibility. Transfer to 3D-printed SM specimens was investigated using only the most promising combination of parameters. The results presented in Fig. 14 confirm that the properties of the cast
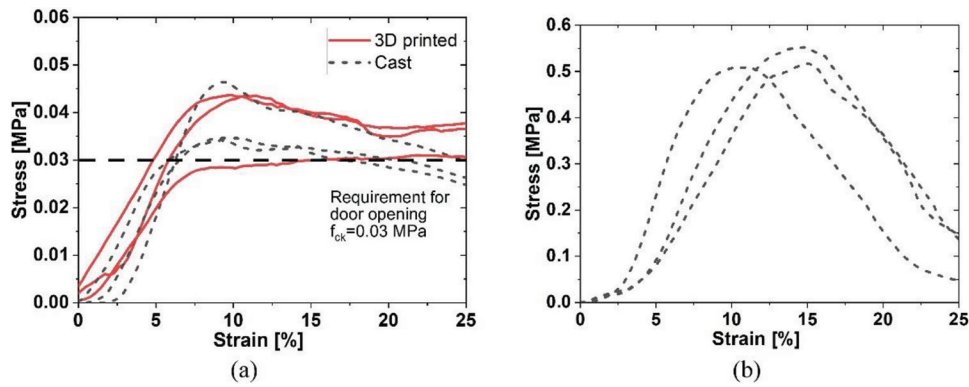
Fig. 14—Stress-strain diagrams of composition M-3, 24 hours after water addition: (a) nonaerated specimens, cured at 60% RH and 20°C for 24 hours; and (b) cast specimens cured in wind channel for 24 hours.

(that is, manually produced SM specimens) match the material properties of the specimens extracted from 3D printed SM layers. Furthermore, it is obvious that aerating the SM for 24 hours indeed enhanced the stress capacity up to 12 times, as shown in Fig. 14.

Sustainability and recyclability

A support structure in 3DCP needs only good short-term properties because it is to be removed after a short time. However, some longer-term properties must nevertheless be considered for the sake of recyclability only. For physical and chemical reasons, dissolving the wood-starch-based SM, preparing it anew with fresh water, and generating fully recycled SM is not an issue. Consolidation and solidification of this type of SM are based on a purely physical process that does not change the chemistry of the substances involved at a molecular level. However, a serious issue in the form of excessive growth of fungi under certain climatic conditions arose 24 hours after SM production (Fig. 15). The SM wall specimen was kept under a normal relative humidity of 50 to 70% and ambient temperature conditions of 20 to 25°C. One side of the SM wall specimen underwent free air circulation—to the right in the image—and the other side—to the left in the photograph—was leaning against a wooden beam that prohibited air circulation. The ESEM images point toward the formation of the "black mildew," also called Aspergillosis. This Aspergillosis species has been reported in some instances to cause serious lung diseases in human beings.[25] For the transfer to practical applications, the wood-starch-based SM mixture should thus contain a fungicide.

SUMMARY AND CONCLUSIONS

Integration of a support material (SM) in extrusion-based additive manufacturing offers a promising solution to produce horizontal and strongly inclined elements. The experimental study demonstrated that wood-starch composites are suitable for continuous three-dimensional (3D) printing of concrete elements. In more detail, the following conclusions can be drawn:

- The mechanical properties of the SM must be adjusted with regard to any particular application scenario—that is, increasing loading imposed by the buildup of the concrete structure. Minimum uniaxial compressive
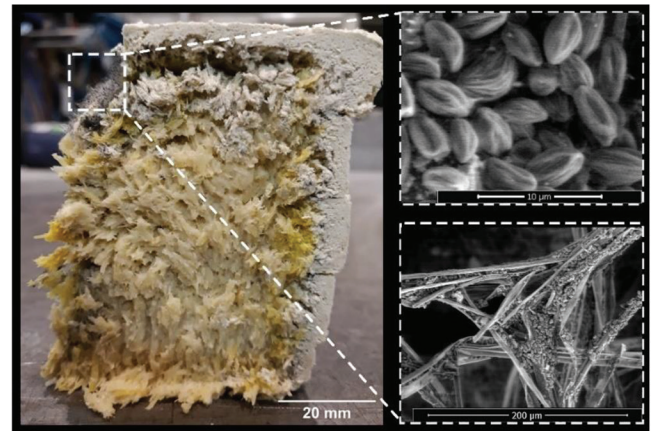

Fig. 15—Fungi formation in 3D printed M-3 SM wall specimen; right side. (Note: scanning electron microscopy images taken at location indicated.)

strength of the SM for a door opening and a window opening were conservatively assessed based on gravity forces exhibited by the subsequently deposited layers. More comprehensive analyses of real loading and deformation conditions of the SM are required, taking into account potential force redistributions and geometrical confinement by adjacent concrete parts.

- Generation of the SM structures should be accomplished by using similar machinery for extrusion of concrete, thus enabling easy SM printing and three-dimensional concrete printing (3DCP) in one continuous process. The experimental campaign revealed that the extrudability of SM was pronouncedly impacted by the extrusion method and SM composition. For screw extruders, it is essential to use SM mixtures with reduced stickiness.

- Accelerated desiccation of the SM by a gentle wind (speed 5 m/s) and slightly decreased relative humidity (50% RH) considerably enhanced the early-age compressive strength of the SM as compared with still air and 60% relative humidity. Although quicker drying supports the buildup of mechanical performance, the high deformability of the freshly placed SM in conjunction with very early mechanical loading remains an issue. In this context, the deformation characteristics

should be investigated under restraint by concomitantly 3D-printed concrete.

- Because intense growth of the fungus "black mildew" was observed approximately 24 hours after extrusion, depending on ambient conditions and the extent of drying, a fungicide should be incorporated into future wood-starch SM recipes.

AUTHOR BIOS

Viacheslav Markin *is a PhD Student in the Department of Civil Engineering, Institute of Construction Materials at Technische Universität Dresden, Dresden, Germany. He received his BSc in 2016 and his MSc in 2018 from Bergische Universität, Wuppertal, Germany. His research interests include the extrusion-based three-dimensional (3D) printing of cementitious materials, environmentally friendly building materials, and methods of mitigating plastic shrinkage of 3D-printed elements.*

Christof Schröfl *has served as the Head of the research group for Morphological and Analytical Characterization at the Institute of Construction Materials at Technische Universität Dresden since 2010. He received his PhD in chemistry from Technische Universität München, München, Germany, in 2010 for his work on polycarboxylate-based high-range water-reducing admixtures for ultra-high-performance concrete. His research interests include the working mechanisms of chemical admixtures and the issues of durability of cement-based composites, including wood-cement composites.*

Paul Blankenstein *is a former Scientific Assistant in the Department of Furniture and Interior Design at the Institut für Holztechnologie, Dresden, Germany. He received his degree from Technische Universität Dresden in 2019. His research interests include the impact of additive manufacturing on materials and fabrication techniques of furniture and building elements.*

Viktor Mechtcherine *has served as a Professor and Director of the Institute of Construction Materials, Faculty of Civil Engineering at Technische Universität Dresden, since 2006.*

ACKNOWLEDGMENTS

REFERENCES

1. Buswell, R. A.; Leal de Silva, W. R.; Jones, S. Z.; and Dirrenberger, J., "3D Printing Using Concrete Extrusion: A Roadmap for Research," *Cement and Concrete Research*, V. 112, Oct. 2018, pp. 37-49. doi: 10.1016/j.cemconres.2018.05.006

2. Buswell, R. A.; da Silva, W. L.; Bos, F. P.; Schipper, H. R.; Lowke, D.; Hack, N.; Kloft, H.; Mechtcherine, V.; Wangler, T.; and Roussel, N., "A Process Classification Framework for Defining and Describing Digital Fabrication with Concrete," *Cement and Concrete Research*, V. 134, Aug. 2020, pp. 1-12.

3. Mechtcherine, V.; Bos, F. P.; Perrot, A.; da Silva, W. L.; Nerella, V. N.; Fataei, S.; Wolfs, R. J. M.; Sonebi, M.; and Roussel, N., "Extrusion-Based Additive Manufacturing with Cement-Based Materials—Production Steps, Processes, and Their Underlying Physics: A Review," *Cement and Concrete Research*, V. 132, June 2020, pp. 1-14. doi: 10.1016/j.cemconres.2020.106037

4. Menna, C.; Mata-Falcón, J.; Bos, F. P.; Vantyghem, G.; Ferrara, L.; Asprone, D.; Salet, T.; and Kaufmann, W., "Opportunities and Challenges for Structural Engineering of Digitally Fabricated Concrete," *Cement and Concrete Research*, V. 133, July 2020, pp. 1-19.

5. De Schutter, G.; Lesage, K.; Mechtcherine, V.; Nerella, V. N.; Habert, G.; and Agusti-Juan, I., "Vision of 3D Printing with Concrete—Technical, Economic and Environmental Potentials," *Cement and Concrete Research*, V. 112, Oct. 2018, pp. 25-36. doi: 10.1016/j.cemconres.2018.06.001

6. Xtree, "XtreeE—3D Printed Wall with Integrated Window Frame," 2019, https://www.youtube.com/watch?v=0byQtXW5Gm8. (last accessed Nov. 5, 2021)

7. ICON—3D Tech, "ICON 3D-Printing for the Homeless in Austin," 2019, https://www.youtube.com/watch?v=is2UVodNphY. (last accessed Nov. 5, 2021)

8. Rudenko, A., "3D-Printed Castle—Photo Gallery," Total Kustom, 2015, http://www.totalkustom.com/photo.html. (last accessed Nov. 5, 2021)

9. Hoffmann, M.; Skibicki, S.; Pankratow, P.; Zieliński, A.; Pajor, M.; and Techman, M., "Automation in the Construction of a 3D-Printed Concrete Wall with the Use of a Lintel Gripper," *Materials (Basel)*, V. 13, No. 8, 2020, pp. 1-15. doi: 10.3390/ma13081800

10. Tay, Y. W. D.; Li, M. Y.; and Tan, M. J., "Effect of Printing Parameters in 3D Concrete Printing: Printing Region and Support Structures," *Journal of Materials Processing Technology*, V. 271, Sept. 2019, pp. 261-270. doi: 10.1016/j.jmatprotec.2019.04.007

11. Molitch-Hou, M., "'Finally, It Stands!' Andrey Rudenko's 3D-Printed Concrete Castle," 2014, https://3dprintingindustry.com/news/finally-stands-andrey-rudenkos-3d-printed-concrete-castle-32097/. (last accessed Nov. 5, 2021)

12. Khoshnevis, B., "Automated Construction by Contour Crafting—Related Robotics and Information Technologies," *Automation in Construction*, V. 13, No. 1, 2004, pp. 5-19. doi: 10.1016/j.autcon.2003.08.012

13. Kondo, H., "3D Printer Support Material: Which One to Use for My Project?" All3DP, 2019, https://all3dp.com/2/3d-printer-support-material-which-one-to-use-for-my-project/. (last accessed Nov. 5, 2021)

14. Ngo, T. D.; Kashani, A.; Imbalzano, G.; Nguyen, K. T. Q.; and Hui, D., "Additive Manufacturing (3D Printing): A Review of Materials, Methods, Applications and Challenges," *Composites Part B: Engineering*, V. 143, June 2018, pp. 172-196. doi: 10.1016/j.compositesb.2018.02.012

15. Duballet, R.; Baverel, O.; and Dirrenberger, J., "Classification of Building Systems for Concrete 3D Printing," *Automation in Construction*, V. 83, Nov. 2017, pp. 247-258. doi: 10.1016/j.autcon.2017.08.018

16. Kaufhold, J.; Kohl, J.; Nerella, V. N.; Schroefl, C.; Wenderdel, C.; Blankenstein, P.; and Mechtcherine, V., "Wood-Based Support Material for Extrusion-Based Digital Construction," *Rapid Prototyping Journal*, V. 4, No. 12, 2019, pp. 690-698. doi: 10.1108/RPJ-04-2018-0109

17. Belitz, H.-D.; Grosch, W.; and Schieberle, P., "Lehrbuch der Lebensmittelchemie: Mit 634 Tabellen," Sechste, Vollständig Überarbeitete Auflage, Springer, Berlin, 2008, 1118 pp.

18. Nerella, V. N.; Näther, M.; Iqbal, A.; Butler, M.; and Mechtcherine, V., "Inline Quantification of Extrudability of Cementitious Materials for Digital Construction," *Cement and Concrete Composites*, V. 95, Jan. 2019, pp. 260-270. doi: 10.1016/j.cemconcomp.2018.09.015

19. Nerella, V. N.; Hempel, S.; and Mechtcherine, V., "Effects of Layer-Interface Properties on Mechanical Performance of Concrete Elements Produced by Extrusion-Based 3D-Printing," *Construction and Building Materials*, V. 205, Apr. 2019, pp. 586-601. doi: 10.1016/j.conbuildmat.2019.01.235

20. Ivaniuk, E., "Investigations on Very Early Strength of 3D-Printable Cementitious Materials," Project Report Submitted in Partial Fulfilment of the Requirement for the Award of the MSc Degree, Technische Universität Dresden, Dresden, Germany, 2019.

21. Ghourchian, S.; Butler, M.; Krüger, M.; and Mechtcherine, V., "Modelling the Development of Capillary Pressure in Freshly 3D-Printed Concrete Elements," *Cement and Concrete Research*, V. 145, July 2021, p. 106457. doi: 10.1016/j.cemconres.2021.106457

22. Perrot, A.; Mélinge, Y.; Rangeard, D.; Micaelli, F.; Estellé, P.; and Lanos, C., "Use of Ram Extruder as a Combined Rheo-Tribometer to Study the Behaviour of High Yield Stress Fluids at Low Strain Rate," *Rheologica Acta*, V. 51, No. 8, 2012, pp. 743-754. doi: 10.1007/s00397-012-0638-6

23. Perrot, A.; Rangeard, D.; Mélinge, Y.; Estellé, P.; and Lanos, C., "Extrusion Criterion for Firm Cement-Based Materials," *Applied Rheology (Lappersdorf, Germany)*, V. 19, No. 5, 2009, p. 53042

24. Khelifi, H.; Perrot, A.; Lecompte, T.; Rangeard, D.; and Ausias, G., "Prediction of Extrusion Load and Liquid Phase Filtration during Ram Extrusion of High Solid Volume Fraction Pastes," *Powder Technology*, V. 249, No. 6, 2013, pp. 258-268. doi: 10.1016/j.powtec.2013.08.023

25. Gordon, S. M., and Avery, R. K., "Aspergillosis in Lung Transplantation: Incidence, Risk Factors, and Prophylactic Strategies," *Transplant Infectious Disease*, V. 3, No. 3, 2001, pp. 161-167. doi: 10.1034/j.1399-3062.2001.003003161.x